Available online at www.sciencedirect.com
ScienceDirect
Journal of Nuclear Materials 363–365 (2007) 600–604
journal of nuclear materials
www.elsevier.com/locate/jnucmat

Impact of bumpiness control on edge plasma in a helical-axis heliotron device

T. Mizuuchi [a,*], S. Watanabe [b], S. Fujikawa [b], H. Okada [a], S. Kobayashi [a], H. Yabutani [b], K. Nagasaki [a], H. Nakamura [b], Y. Torii [a], S. Yamamoto [c], M. Kaneko [b], H. Arimoto [b], G. Motojima [b], H. Kitagawa [b], T. Tsuji [b], M. Uno [b], S. Matsuoka [b], M. Nosaku [b], N. Watanabe [b], Y. Nakamura [b], K. Hanatani [a], K. Kondo [b], F. Sano [a]

[a] *Institute of Advanced Energy, Kyoto University, Gokasho, Uji 611-0011, Japan*
[b] *Graduate School of Energy Science, Kyoto University, Gokasho, Uji 611-0011, Japan*
[c] *Graduate School of Engineering, Osaka University, 1-1 Yamadaoka, Suita 565-0871, Japan*

Abstract

In the helical-axis heliotron configuration, bumpiness of the confinement field ε_b is introduced to control the plasma transport. The plasma performance were experimentally investigated in Heliotron J for three configurations with $\varepsilon_b = 0.01$, 0.06 and 0.15 at $\rho = 2/3$. The obtained volume-averaged stored energy depends on the configuration. To understand the observed difference in global energy confinement, the ε_b-control effects on the edge plasma is discussed. For $\varepsilon_b = 0.01$, the plasma density and temperature in the peripheral region is low compared to other cases. This poor plasma edge relates to the observed low stored energy or poor energy confinement for $\varepsilon_b = 0.01$.

PACS: 52.55.Hc; 52.40.Hf; 52.25.Xz; 52.30.Ex

Keywords: Heliotron J; Bumpiness control; Helical-axis heliotron

1. Introduction

In stellarator/heliotron devices, the control of ripple loss is a key issue from the viewpoint of neoclassical transport. In the helical-axis heliotron concept [1], bumpiness, ε_b, of the Fourier components in Boozer coordinates [2] is introduced as a third measure to control the neo-classical transport in addition to conventional two components, toroidicity, ε_t, and helicity, ε_h. The role of bumpiness is to align the mod-B_{min} contours with the magnetic flux surfaces [3]. Heliotron J [4–6] is a flexible low-magnetic-shear helical-axis heliotron device with a continuous $L = 1/M = 4$ helical field coil (L, the pole number of the helical coil and M, the helical pitch). This device has four mirror-like sections along the

* Corresponding author. Tel.: +81 774 38 3451; fax: +81 774 38 3535.
E-mail address: mizuuchi@iae.kyoto-u.ac.jp (T. Mizuuchi).

0022-3115/$ - see front matter © 2007 Elsevier B.V. All rights reserved.
doi:10.1016/j.jnucmat.2006.12.036

torus. In the middle of each mirror-like section, the configuration is designed to produce almost no toroidal curvature and nearly constant magnetic-field strength across the plasma. Therefore, a quasi-isodynamic configuration can be realized and the deviation of the orbits of high pitch-angle particles from the magnetic surface can be kept small. One of the main objectives of the Heliotron J experiment is to examine the ε_b-control effects on the plasma performance from the viewpoint of not only neoclassical but also anomalous transport.

Recently, effects of ε_b-control on the plasma performance have been investigated in Heliotron J by selecting three configurations with $\varepsilon_b = 0.01$, 0.06, and 0.15 at $\rho = 2/3$ under the condition of almost the same edge rotational transform ($\iota(a)/2\pi \approx 0.558$–$0.562$) and plasma volume (0.68–0.75 m^3) [7]. The experiment shows that the higher bumpiness configuration seems to be preferable for the confinement of fast-ions produced by NBI/ICRF in ECH target plasmas [8,9]. However, for the bulk plasmas, as shown in Fig. 1, the volume-averaged plasma stored energy W_p^{dia}/V_p is higher in the case of $\varepsilon_b = 0.06$ than that in the $\varepsilon_b = 0.15$ case at the same line-averaged density. The lowest W_p^{dia}/V_p is observed in the lowest ε_b case. These properties of the bulk plasma performance become more evident in higher density region.

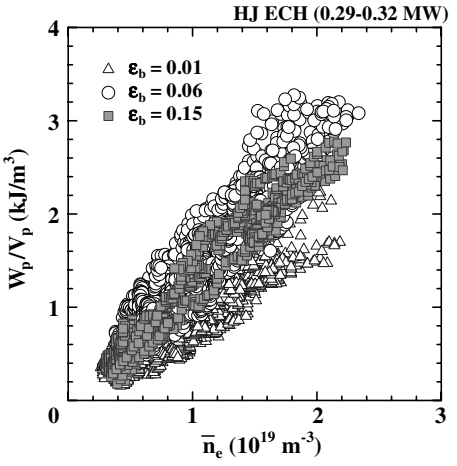

Fig. 1. Density dependence of the volume-averaged plasma stored energy density W_p^{dia}/V_p.

When the global energy confinement time normalized by the ISS04 scaling [10], $\tau_E^{exp}/\tau_E^{ISS04}$, is compared [7], the highest value is again observed in the $\varepsilon_b = 0.06$ configuration. Here, the radiation-loss power was neglected in the estimation of τ_E^{exp}. In the inter-machine (or inter-configuration) confinement scaling in helical systems, ISS04, the effective helical ripple modulation amplitude, ε_{eff}, has been proposed as an additional parameter of the scaling [10]. Although the concept of ε_{eff} is originally based on the neoclassical transport viewpoint, the effect of this parameter on the suppression of turbulence dominant transport is discussed. It is expected that lower ε_{eff} is preferable to the confinement. From this point of view, the observed difference in $\tau_E^{exp}/\tau_E^{ISS04}$ for the three configurations in Heliotron J seems to be qualitatively consistent with this expectation [7] since the smallest ε_{eff} is obtained in the $\varepsilon_b = 0.06$ configuration and the largest one is obtained in the $\varepsilon_b = 0.01$ configuration as shown in Table 1.

In the study of the configuration effect on the global confinement property, we should pay attention to the change in the edge plasma parameters. The stored energy in the edge region could have a lot of contribution to the volume-averaged stored energy. On the other hand, the difference in the proximity of plasma to the PFM surfaces among the configurations could directly or indirectly affect the edge or whole plasma performance through PSI effects. In helical devices, there are some reports on the difference in edge plasma structure relating to the L- and H-mode transition phenomena in the same configuration [11,12]. The difference in the proximity to PFM is listed up as a candidate to explain lower plasma performances observed in some configuration studies [13]. However, the systematic

Table 1
Parameters of magnetic configuration

I_{TA}/I_{TB}	($\rho = 2/3$)			$\lvert B\rvert$ (T)	R (m)	$\langle a\rangle$ (m)	$\iota/2\pi$ ($\rho = 1$)	$\iota/2\pi$ ($\rho = 2/3$)	Well (%) ($\rho = 2/3$)	ε_{eff}
	ε_b B_{04}/B_{00}	ε_h B_{14}/B_{00}	ε_t B_{10}/B_{00}							
5/3	0.01	−0.141	−0.099	1.193	1.200	0.170	0.562	0.554	0.39	0.258
5/2	0.06	−0.125	−0.102	1.261	1.197	0.171	0.561	0.553	0.95	0.135
5/1	0.15	−0.128	−0.108	1.362	1.185	0.180	0.558	0.539	0.82	0.221

$\lvert B\rvert$: the averaged magnetic-field strength along the magnetic-axis, ε_{eff}: the effective ripple modulation amplitude at $\rho = 2/3$.

experiments on the relationship between the global confinement and edge plasma properties in different configurations of helical devices are not reported. This paper reports the differences of the edge plasma structure observed in the ε_b-control experiment.

2. Experiment and characteristics of edge field configuration

The details of the ε_b-control experiment in Heliotron J are described in [7], where the current ratio of two toroidal field coil sets (TFC-A and TFC-B), I_{TA}/I_{TB}, is mainly controlled to change ε_b. In order to achieve the on-axis heating condition for 70 GHz second harmonic ECH, the magnetic-axis position and the magnetic-field strength on the minor-axis are required to be constant at the ECH launching section, which is located in the middle of a mirror-like section [4]. Due to this restriction, the averaged field strength along the magnetic-axis has to be increased in a higher bumpiness configuration. We selected three configurations; $\varepsilon_b = 0.15$, 0.06 and 0.01 at $\rho = 2/3$ in the vacuum condition. Since the $\iota(a)/2\pi$-scan experiments have shown the strong effects of $\iota(a)/2\pi$ on the plasma confinement [13,14], the edge rotational transform is maintained nearly constant ($\approx$0.558–0.562) in the vacuum condition. Some parameters for the magnetic configurations are listed in Table 1.

The magnetic surfaces do not intersect the wall and no clear magnetic-island chain is observed both in the core and edge regions for all configurations. However, the gap between LCFS and the wall in the inboard side at the end of the mirror-like section (high field side) is short for $\varepsilon_b = 0.15$ (see Fig. 4(a)). Fig. 2 shows the connection length of the SOL field lines to the wall as a function of the distance from LCFS, $\Delta\ell$. Here, the field lines start along the scanning line of the SOL probe. The connection length gradually decreases from 50–100 m to $\sim$10 m as increase of $\Delta\ell$ and then suddenly drops to less than $\sim$3 m at $\Delta\ell \sim 2$ cm for $\varepsilon_b = 0.01$ and 0.15, and at $\Delta\ell \sim 3$ cm for $\varepsilon_b = 0.06$. The relatively short connection length is observed for $\varepsilon_b = 0.15$ maybe due to the inward shift of the confinement region at the ends of the mirror-like section and the relatively lager plasma radius.

3. Bumpiness control effects on edge plasmas

The effects of bumpiness on the plasma performance are investigated for ECH plasmas ($\bar{n}_e \sim$ 0.2–2.5 $\times$ 1^{19} m^{-3}, $T_e \sim$ 0.3–1 keV, $P_{ECH} = 0.29$–0.32 MW). The profiles of the edge plasma density, temperature, and floating potential were measured with a set of Langmuir probes (SOL probe) on a shot-by-shot basis. Fig. 3 shows the SOL plasma profiles for low-density ($\sim 0.4 \times 10^{19}$ m^{-3}) ECH plasmas as a function of $\Delta\ell$ in the three configurations ($\varepsilon_b = 0.01$, 0.06, 0.15). The space potential V_s estimated by $V_s \approx V_f + 3 \times T_e$ and the particle flux $\tilde{\Gamma}_{turbu}$ caused by the edge plasma turbulence, which is estimated by the same method in Ref. [15], are also plotted.

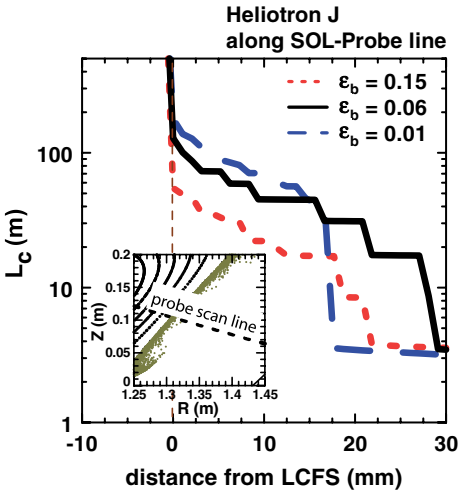

Fig. 2. Connection length of the SOL field lines to the wall as a function of $\Delta\ell$. The inset indicates the probe scanning line.

The floating potential V_f in the region far from LCFS (30–40 mm) is about 10 V in all cases. Approaching the core plasma, V_f starts to increase gradually, and then decreases at a position near LCFS and finally goes down to negative values. The position of this inflection point of V_f-profile is $\Delta\ell \sim 5$ mm outside LCFS for $\varepsilon_b = 0.01$ and 0.15, but $\Delta\ell \sim 10$ mm outside LCFS for $\varepsilon_b = 0.06$. The steepest drop of V_f is observed in the case of $\varepsilon_b = 0.15$ and the gentlest drop is observed in the case of $\varepsilon_b = 0.01$. The gradients of I_s- and T_e-profiles also change near the inflection point of V_f-profile. The gradients of T_e- and I_s-profiles inside the inflection point become steep. The change of the gradient becomes larger with increase of ε_b.

A hump in the T_e-profile is observed at $\Delta\ell \sim$ 14 mm for $\varepsilon_b = 0.15$ as shown in Fig. 3. The V_s-profile also has a hump due to this hump in T_e-profile and indicates the existence of E_r-shear. Although the effect on $\tilde{\Gamma}_{turbu}$ is not clear in this figure, these

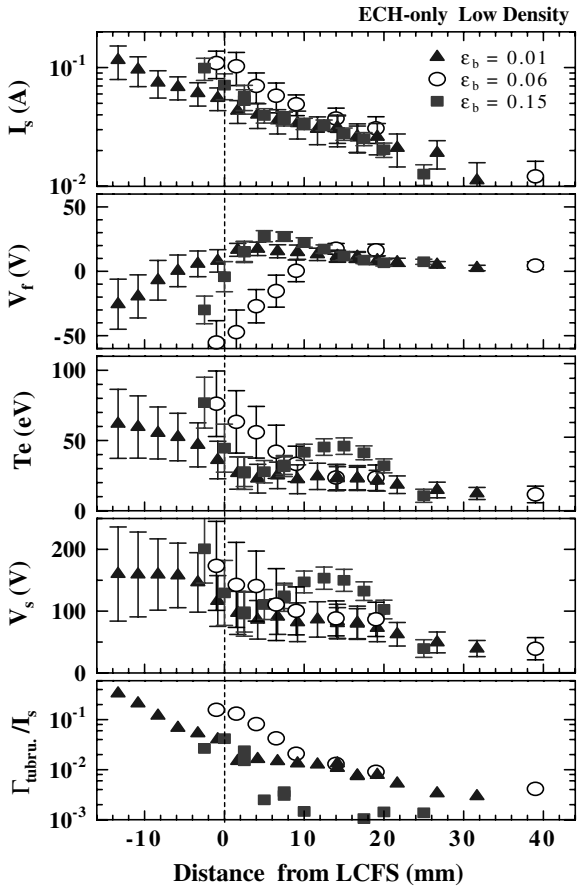

Fig. 3. SOL plasma profiles for low-density ($\sim 0.4 \times 10^{19}\ m^{-3}$) ECH plasmas as a function of $\Delta\ell$.

observations are interesting relating from the viewpoint of suppression of SOL plasma turbulences. It is one of important subjects in near future experiments to study the mechanism of the hump and its effect on edge plasma transport.

As shown in Fig. 3, the values of T_e and I_s just inside LCFS are significantly low. (Due to such a low-density and low-temperature edge, the probe could be inserted deeply inside LCFS without severe damage on the discharge only in this configuration. For other configurations, the insertion of the probe was limited up to ~2–3 mm inside LCFS even in this low-density case.) Such a low-density and temperature edge might have relation to the observed low W_p^{dia} in this configuration. It is interested to check whether such a relatively low-density and temperature edge in the low bumpiness configuration is observed also for higher density plasmas. Unfortunately, the probe measurement was limited outside LCFS for higher density plasmas, therefore, we try to discuss this point by using a radiation profile from a SX photo-diode array. Fig. 4(a) shows the sight lines of the array with LCFS for the three configurations. Since the shape of LCFS in the large-R side is smooth as compared to that in the small-R side, we checked the radial profiles of chord-integrated intensity only in this large-R side.

Fig. 4(b) and (c) shows the radial profiles of chord-integrated intensity from the array for low

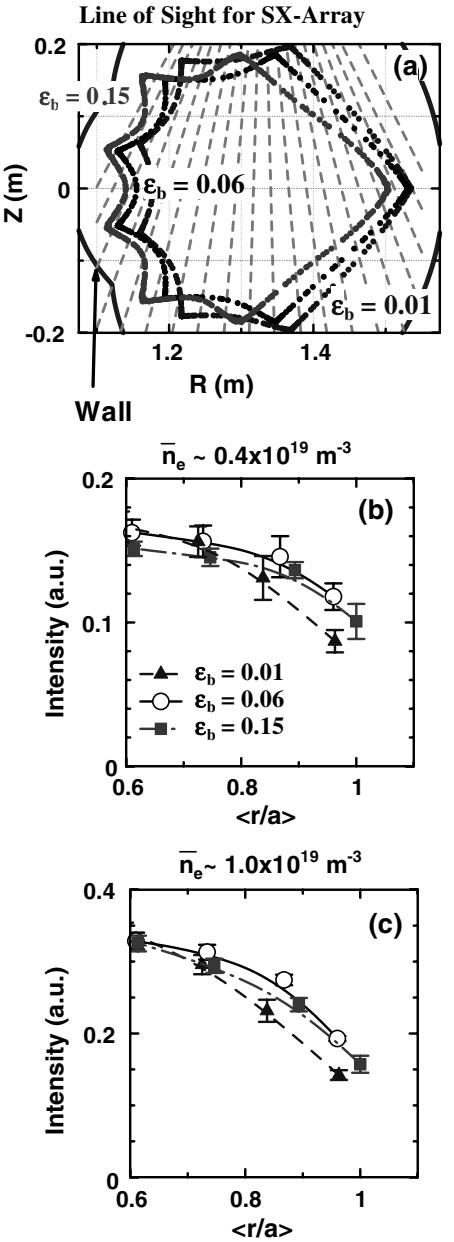

Fig. 4. (a) Sight lines of the SX photo-diode array. The radial profiles of chord-integrated intensity for (b) low ($\sim 0.4 \times 10^{19}\ m^{-3}$) and (c) medium ($\sim 1 \times 10^{19}\ m^{-3}$) density discharges.

($\bar{n}_e \sim 0.4 \times 10^{19}$ m^{-3}, Fig. 4(b)) and medium ($\bar{n}_e \sim 1 \times 10^{19}$ m^{-3}, Fig. 4(c)) density discharges. The low-density case is taken from the same discharge set as that for Fig. 3. The intensity of the radiation in the edge region for the $\varepsilon_b = 0.01$ case is clearly lower than that in other two cases. This is qualitatively consistent with the expectation from the probe data. The similar difference in the edge radiation profile is also observed in the medium density discharge as shown in Fig. 4(c), suggesting relatively low-density and temperature in the peripheral region of the $\varepsilon_b = 0.01$ configuration. Even in this configuration, a spontaneous transition like the H-mode [13] is observed for higher density discharge [7]. In such a phase, the change of the radiation profile indicates some improvement of the edge plasma performance and then the increase of the stored energy can be observed. The global energy confinement, however, stays in a low value.

Although the steepest gradient of the SOL plasma profile is observed in the $\varepsilon_b = 0.15$ configuration from the SOL probe data, the difference in the radiation profile inside LCFS between the $\varepsilon_b = 0.06$ and 0.15 configurations is not clear. Therefore the observed difference in plasma performance between these two configurations might not be explained by the degradation of edge plasma parameter, which is observed in the $\varepsilon_b = 0.01$ configuration. Since the gap between LCFS and PFM is small in the $\varepsilon_b = 0.15$ configuration, the increase of plasma–material interaction or resultant increase of radiation-loss might have more important effects on the global energy confinement in this configuration. Unfortunately, we have no absolute measurement of radiation power and we cannot make quantitative discussions on the radiation-loss effects in the power balance at present. It should be necessary to take into account the radiation-loss in the detailed discussions of the ε_b-effect (or the ε_{eff}-interpretation) on the global energy confinement.

4. Summary

Effects of the bumpiness control on the plasma performance were investigated in Heliotron J by selecting three configurations with $\varepsilon_b = 0.01$, 0.06, 0.15 at $\rho = 2/3$, almost the same edge rotational transform and plasma volume. In order to understand the observed bumpiness effect on the global energy confinement for ECH plasmas, the effects of the bumpiness control on the edge plasmas are discussed.

For the $\varepsilon_b = 0.01$ configuration, it is experimentally confirmed that the plasma density and temperature in the peripheral region are low compared to those in other cases. Although it is not clear at present why such an edge plasma structure is realized only in this configuration, it is considered that such a poor plasma edge relates to the lower stored energy or poorer energy confinement in this configuration.

In order to explore further experimental optimization of the helical-axis heliotron concept by utilizing the bumpiness control, it is necessary to understand the mechanism which induce the observed edge plasma structure for each configuration. Moreover, detailed evaluation of the effects of PSI on the plasma performance is also necessary to extract only the configuration control effect on the plasma transport.

Acknowledgements

The authors are grateful to the Heliotron J supporting group for their excellent arrangement of the experiments. This work is supported by the Collaboration Program of the Laboratory for Complex Energy Processes, IAE, Kyoto University, the Kyoto University 21st-century COE Program and the National Institute of Fusion Science Collaborative Research Program (NIFS04KUHL001∼008).

References

[1] M. Wakatani et al., Nucl. Fusion 40 (2000) 569.
[2] A.H. Boozer, Phys. Fluids 23 (1980) 904.
[3] M. Yokoyama et al., Nucl. Fusion 40 (2005) 261.
[4] T. Obiki et al., Nucl. Fusion 39 (1999) 1667.
[5] F. Sano et al., J. Plasma Fusion Res. Ser. 3 (2000) 26.
[6] T. Obiki et al., Nucl. Fusion 41 (2001) 833.
[7] T. Mizuuchi et al., Fusion Sci. Technol. 50 (2006) 352.
[8] M. Kaneko et al., Fusion Sci. Technol. 50 (2006) 428.
[9] H. Okada et al., Fusion Sci. Technol. 50 (2006) 287.
[10] H. Yamada et al., Fusion Sci. Technol. 46 (2004) 82.
[11] F. Wagner et al., Plasma Phys. Control. Fusion 36 (7A) (1994) A61.
[12] K. Toi et al., Phys. Plasmas 12 (2005) 0207011.
[13] F. Sano et al., Nucl. Fusion 45 (2005) 1557.
[14] T. Mizuuchi et al., J. Plasma Fusion Res. 81 (2005) 949.
[15] T. Mizuuchi et al., J. Nucl. Mater. 337–339 (2005) 332.